Container material dictates stability of bacteriophage suspensions: Light scattering and infectivity measurements reveal mechanisms of infectious titre decay

Larry O'Connell, Yoann Roupioz, Pierre R Marcoux

O'Connell Larry (Orcid ID: 0000-0002-9551-3444)
Marcoux Pierre R. (Orcid ID: 0000-0003-3855-9662)

Container Material Dictates Stability of Bacteriophage Suspensions: Light Scattering & Infectivity Measurements Reveal Mechanisms of Infectious Titer Decay

Larry O'Connell[1,2], Yoann Roupioz[2], Pierre R. Marcoux[1,*]

[1] Univ. Grenoble Alpes, CEA, LETI, F-38054 Grenoble, France

[2] Univ. Grenoble Alpes, CNRS, CEA, IRIG, SyMMES, F-38000 Grenoble, France

*Correspondance: pierre.marcoux@cea.fr; Tel.:+33-4-38-78-15-04

Keywords: Bacteriophage, colloidal stability, aggregation, virus adsorption, nanoparticle tracking analysis, infectious titer, phage stability, plaque counting

Abbreviated running headline: Mechanisms of Infectious Titer Loss

Abstract

Aims: To measure the infectious titer (IT) decay rate for various bacteriophages as a function of storage container material. Additionally, parallel light scattering and infectious titer measurements reveal distinct mechanisms for IT loss, depending on phage.

Methods and Results: Suspensions of bacteriophages 44AHJD, P68, and gh-1 were stored in various labware. IT of each suspension was repeatedly measured over the course of two weeks. Large variability in IT decay was observed, with $>4\ \log_{10}$ loss in glass and low-binding polypropylene. Incubation of polymer containers with Bovine Serum Albumin (BSA) resulted in a consistent reduction in IT decay. Aggregation state of phage suspensions was studied by nanoparticle tracking analysis

This article has been accepted for publication and undergone full peer review but has not been through the copyediting, typesetting, pagination and proofreading process which may lead to differences between this version and the Version of Record. Please cite this article as doi: 10.1111/jam.15581

(NTA), revealing highest aggregation in glass-stored suspensions and lowest after storage in BSA-treated containers.

Conclusions: Glass and "low-binding" containers may aggravate IT decay while BSA treatment may present an easy mitigation strategy. IT *vs.* NTA titer diagrams highlight the importance of phage inactivation in combination with aggregation.

Significance and Impact of the Study: Container material is a significant determinant of bacteriophage IT decay. It is therefore essential to confirm IT following storage and tailor choice of phage storage containers accordingly. Aggregation of phages and adsorption onto labware surfaces are not the only mechanisms accounting for IT loss, but also biological instability.

Introduction

Bacteriophages (phages) have been employed in a remarkable variety of applications (O'Connell *et al.*, 2021) including *in vivo* treatment of pathogenic bacteria (Kakasis and Panitsa, 2019), as a vaccine vector (Staquicini *et al.*, 2021), and as surrogates for the study of eukaryotic viruses in water remediation facilities (Hu *et al.*, 2003; Langlet *et al.*, 2008) and SARS-CoV-2 survival in microdroplets (Fedorenko *et al.*, 2020). In each of these contexts it is essential to understand any changes in particle size and concentration that may occur; be it through aggregation, inactivation, adsorption onto labware surfaces, or some other effect that causes an evolution of the measured infectious titer. This is especially true in a clinical context involving preparation and administration of phage preparations, since regulatory agencies standardize therapeutic doses based on the number concentration of phage ml^{-1} of such suspensions. So-called magistral preparations can have infectious titer on the order of 10^{10}-10^{12} PFU ml^{-1} (Ferry *et al.*, 2018), before being diluted to 10^{5} – 10^{7} PFU ml^{-1} for administration to a patient (Wright *et al.*, 2009; Biswas *et al.*, 2018; Jault *et al.*, 2018).

Infectious titer (IT) is measured through the observation and counting of lysis plaques in a host bacterial lawn in soft agar (Perlemoine *et al.*, 2021). IT decay during storage or processing can have profound effects on downstream applications if the reduction is not mitigated or compensated for. In a published clinical trial, a failure to take into account a decay of infectious titer of phage suspensions resulted in patients receiving a dose of 10^{2}-10^{3} PFU ml^{-1} instead of the intended 10^{6} PFU ml^{-1}, due to an unanticipated 3 $\log_{10}$ drop in IT of phage preparations over the course of 15 days in storage (Jault *et al.*, 2018). In wastewater remediation, over-estimation of the viral elimination capability of water purification processes may result from reduction in infectious titer and/or aggregation of phage which inadvertently increases filtration performance (Langlet *et al.*, 2008). In survival studies of SARS-CoV-2 virus in respiratory droplets, aggregation of bacteriophage (employed as surrogate viral particles) is recognized as a potential confounding factor for interpretation of survival estimates (Fedorenko *et al.*, 2020).

Recently, it was revealed that exposure to common labware can lead to a drastic reduction of bacteriophage infectious titer on timescales ranging from days to mere hours (Richter *et al.*, 2021). Three mechanisms can cause the observed IT losses: adsorption onto labware surfaces, virion aggregation in the aqueous phase, and finally virus inactivation. These phenomena have important implications, not only for future phage research, but also in retrospect when considering findings of past publications that may have failed to control for such an effect. As a result, there is now interest in treatment of container surfaces (Wdowiak *et al.*, 2021) and optimization of phage buffer composition (Duyvejonck *et al.*, 2021) to mitigate loss of infectious titer.

The present work explores the phenomenon of phage infectious titer loss in common glass and polymer labware, extending the investigation to three new phages that have not been previously investigated. Furthermore, in addition to standard counting of lysis plaques, light scattering analysis of virus suspensions was performed. Nanoparticle tracking analysis (NTA) reveals the aggregation state of phage suspensions as a function of storage container material and was compared to changes in infectious titer as measured by the drop cast method (Chhibber *et al.*, 2018). Finally, pre-incubation of container surfaces with amphiphilic protein bovine serum albumin (BSA) is demonstrated as a simple and effective method for significantly reducing IT loss. Scanning electron microscopy was performed on container surfaces in order to assess the level of phage surface adsorption.

Materials and methods

Host bacterium and bacteriophage preparation

Bacterial hosts *Staphylococcus aureus* subsp. *aureus* Rosenbach (ATCC 43300; host of phage 44AHJD) and *Staphylococcus aureus* (ATCC BAA-2312; host of phage P68) were obtained from Microbiologics (Kwik-Stik™ lyophilized strains). *Pseudomonas putida* (ATCC 12633; host of phage gh-1), phages 44AHJD (Rosenblum and Tyrone, 1964), P68, and gh-1 (Lee and Boezi, 1966) were obtained from the *Félix d'Hérelle Reference Center for Bacterial Viruses* of the Université Laval, Quebec, Canada. All three phages used in this work are lytic, non-enveloped members of the *Podoviridae* family. Electron microscopy has indicated a 75 nm icosahedral head for both 44AHJD and P68 with a short, non-contractile tail of ~27 nm in length for 44AHJD and ~40 nm in length for P68. (Vybiral *et al.*, 2003) Phage gh-1 features a 50 nm icosahedral head with a ~10 nm tail. (Lee and Boezi, 1966)

Bacterial cultures were routinely prepared in recommended media. *S. aureus* ATCC 43300 was cultured in Soybean Casein Digest Broth TSB (Sigma-Aldrich, Saint Quentin Fallavier, France) at 37 °C; *S. aureus* ATCC BAA-2312 in ATCC Medium 3 (Supporting Information) at 37 °C; *Pseudomonas putida* in ATCC Medium 18 at 30 °C.

Bacteriophage suspensions were routinely prepared using the soft overlay agar method (Adams, 1959). 100 µl of overnight liquid precultures of each bacterial host were inoculated into fresh medium and allowed to proliferate until reaching 10^8 CFU ml^{-1} as confirmed by optical density at 550 nm. Then, 200 µl bacterial host and 100 µl bacteriophage suspension (5×10^4 PFU ml^{-1} for 44AHJD, 5×10^3 PFU ml^{-1} for P69 and gh-1) were inoculated into 15 ml falcon tubes filled with 5 ml molten agar (TSB prepared with 7.5 g l^{-1} agar (Sigma-Aldrich, Saint Quentin Fallavier, France)) at 51.5 °C, vortexed, and poured over 20 ml solidified tryptic soy agar (TSA, 15 g l^{-1} agar) in a standard 90 mm petri plate (VWR, France). Plates were then incubated overnight until lysis plaques became confluent in the top agar layer, which was then collected and soaked for 4 h at room temperature in sterile

154 mmol l^{-1} NaCl solution (OTEC, VWR) in a 50 ml polypropylene tube. Each tube was then twice centrifuged for 20 min 5500 *g* at 4 °C and the supernatant retained each time.

Each suspension was brought to 0.5 mol l^{-1} NaCl and 8% w/v polyethylene glycol 6 kDa (Merck, Darmstadt, Germany) and left at 4 °C overnight. The following day, each suspension was centrifuged for 30 min at 12108 *g* at 4 °C, the supernatant removed, and the pellet resuspended in sterile 154 mmol l^{-1} NaCl, vortexed, centrifuged 20 min 5500 *g* at 4 °C and the supernatant retained.

Deionized water (>18 MΩ resistivity) was obtained from an ELGA PURELAB flex dispenser (Veolia Water, France). Phage suspensions were then purified by ultracentrifugation for 2 h at 100,000 *g* at 4 °C on a CsCl (VWR) step gradient (1.7 g ml^{-1}, 1.54 g ml^{-1}, and 1.34 g ml^{-1} CsCl in deionized water) in 5 ml, Open-Top Thinwall Ultra-Clear ultracentrifuge tubes (Beckman Coulter, Villepinte, France) in a SW55Ti swinging-bucket rotor (Beckman Coulter) mounted in an Optima l-90K Ultracentrifuge (Beckman Coulter). Bacteriophages were concentrated at the second visible band from the top and collected with a micropipette. CsCl was removed from phage suspensions by repeated ultrafiltration and resuspension in 154 mmol l^{-1} NaCl using 100 kDa Vivaspin 500 ultrafiltration units (Sartorius).

Container preparation

Sterile 10% w/v BSA stock solution was prepared by dissolving 100 mg BSA (Sigma-Aldrich, Saint Quentin Fallavier, France) in 10 ml 154 mmol l^{-1} NaCl solution followed by filter sterilization through a 0.2 µm syringe filter (Millipore, Cork, Ireland). This stock solution was diluted to 0.1% w/v BSA before use.

Clear 2 ml borosilicate glass vials (Wheaton, Dutcher. Reference 048398) were autoclaved six days before use and stored in a sterile hood at room temperature. These tubes were chosen due to their low levels of extractables and low potential for leaching of contaminants into the phage suspension. 1.5 ml polypropylene (PP) tubes (Eppendorf, VWR) were autoclaved >48 h before use. 1.5 ml low protein-binding polypropylene (PP LoBind) tubes (Protein LoBind, Eppendorf, VWR) were autoclaved >48 h before use. Sterile 15 ml polystyrene (PS) tubes (Falcon, UGAP, France. Reference 2515477) were used without any prior treatment. To produce BSA-treated containers, 1.5 ml polypropylene tubes (autoclaved >48 h before use) and 15 ml polystyrene tubes were incubated upright overnight at 4 °C

with 0.1 % BSA solution. The following morning, all tubes were inverted to coat the upper interior surface for a further 6 h. PP+BSA and PS+BSA tubes were then emptied and rinsed thoroughly with 154 mmol l^{-1} NaCl and emptied shortly before addition of phage suspensions.

Serial dilution of phage suspensions

For each container type, each of the three phage suspensions were serially ten-fold diluted ten times, producing 10^{-1} to 10^{-10} dilutions. For suspensions stored in glass, PP, and PP+BSA containers: suspensions were diluted 100 µl in 900 µl 154 mmol l^{-1} NaCl. For suspensions stored in 15 ml PS and PS+BSA containers: suspensions were diluted 1 ml in 9 ml 154 mmol l^{-1} NaCl due to the larger tube size.

Phage titer enumeration

Infectious titer was measured using the drop cast method: a bacterial lawn was prepared by inoculating 200 µl of an overnight liquid preculture of each bacteriophage's respective host into 5 ml of molten agar at 51.5 °C (tryptic soy broth containing 7.5 g l^{-1} agar) and then poured over 20 ml solid TSA (15 g l^{-1} agar) in a standard petri dish. Once the bacterial agar layer cooled and solidified for a few minutes, 10 µl drops of each phage dilution were placed on the bacteria-inoculated agar layer. The droplets are allowed to dry before incubating the plates at the appropriate temperature for each host. Phage lysis plaques were then counted manually after a few hours and then a second time the following day. This two-step counting is performed since lysis plaques can overlap with each other and become indistinguishable if left for too long while counting too early results in late-starting plaques being missed. All phages used in this work produced well-defined, clear plaques, which facilitated counting. Phage suspensions were titered at the following timepoints: after 5 min (*i.e.*, immediately after the initial dilution), 24 h, 48 h, 1 week, and 2 weeks.

Since it has been demonstrated that agitation of phage suspensions can have a strong effect on titer decay (Trouwborst *et al.*, 1974; Rossi and Aragno, 1999), care was taken to vortex all tubes an identical duration of only 5 seconds prior to plating. All tubes were stored upright in the dark at 4 °C in between measurements. A correction factor was applied to the observed count of lysis plaques to

compensate for overlap bias (Howes, 1969; Howes and Fazekas de St Groth, 1969) (See Supporting Information).

Nanoparticle tracking analysis

Nanoparticle tracking analysis (NTA) was carried out using a Nanosight NS300 (Malvern Pananalytical Ltd., Malvern, United Kingdom) fitted with a 488 nm laser module and a sCMOS detector. Samples were diluted with 154 mmol l^{-1} NaCl to produce suspensions of 10^8-10^9 particles ml^{-1}, and the dilution factor noted. Each sample was injected by syringe pump into the analysis chamber and measured five times with each measurement lasting 60 s, according to the manufacturer's protocol. All suspensions were analysed with a consistent camera level of 16 and detection threshold of 10. Preliminary data processing was performed using NTA Analytical software (v3.4.4). Violin plots were produced using the violins.m function (Bechtold, 2016) in MatLab R2021a (v9.10). This data representation presents smoothed vertical histograms of size spectra, each inset with a box-and-whisker plot displaying the median, lower and upper quartiles, and the minimum and maximum of the distribution (Hintze and Nelson, 1998).

Contact angle measurements

Contact angle measurements were performed on replicates of all containers using a GBX Digidrop (Tallaght, Ireland). Replicates of all containers were freshly prepared precisely as before, dried with compressed air, broken into small sections, placed on the Digidrop stage, and had 1.5 µl deionized water dispensed on the surface with a micropipette. All contact angle images were analysed using the Contact Angle plugin implemented in the FIJI distribution of ImageJ v1.53c (Schindelin *et al.*, 2012).

Electron microscopy

Scanning electron microscopy (SEM) was performed on a selection of containers. Each container was cut open to expose the interior surface. In order to avoid charging effects during imaging, a ~4 nm layer of carbon was deposited on the tube interiors using a Safematic CCU-010 HV compact coating unit (Zizers, Switzerland), at 3×10^{-5} mBar, with the sample mounted at stage height 6. The surface was observed in a Zeiss ultra 55 scanning electron microscope under a 2 kV acceleration voltage and 4-10 mm working distance.

Statistical Analysis

A separate Kruskal-Wallis H test1 was performed for each phage to determine if storage container had an influence on proportion of infectious titer remaining after 14 days of storage.

Results

As purified bacteriophage suspensions are routinely processed and stored from days to months in polymer and glass labware before use, infectious titers of highly purified phage preparations were measured in this work at intervals over the course of two weeks, revealing a time-dependency of infectious titer decay as a function of container material. Glass, polystyrene, polypropylene, and low-binding polypropylene were studied, since use of these materials is common practise in microbiology labs worldwide. All phage suspensions were constituted with pyrogen-free, 0.2 µm-filtered, sterile saline (0.9% w/v NaCl solution (OTEC, VWR)). Addition to the buffer of tris and divalent cations was avoided in order to render the results more universally applicable, considering the variety of phage buffers commonly used in microbiology labs. Furthermore, phage stability exhibits large variation depending on solution composition (Duyvejonck *et al.*, 2021). Addition of PEG or other protectants was avoided in order to isolate the effects of container surface interaction with the three phages studied.

A dramatic drop in infectious titer was observed for all three phages stored in almost all containers except those treated with BSA (Figure 1). These results are summarized in Table S1. Storage in glass vials results in significant loss of infectious titer for all three phage: 3.67 $\log_{10}$ loss of 44AHJD, 3.4 $\log_{10}$ loss of P68 and 2.4 $\log_{10}$ loss of gh-1. Titer decay progresses very quickly for phages 44AHJD and P68, but in the case of gh-1 remains comparatively stable for the first two days before showing similar exponential decay. Storage in PP resulted in over 3.11 $\log_{10}$ loss of 44AHJD and 3.47 $\log_{10}$ loss of P68 but resulted in less dramatic loss of 1.54 $\log_{10}$ of gh-1. Incubation of PP with BSA improved retention relative to untreated PP by between 1.31 and 2.40 $\log_{10}$, depending on phage. Low protein-binding PP tubes, marketed under the name 'Protein LoBind', resulted in dramatically different IT decay depending on phage, with only 0.8 $\log_{10}$ loss of 44AHJD, but 4.65 $\log_{10}$ loss of P68 and 4.22 $\log_{10}$ loss of gh-1. In the latter case of P68 and gh-1, PP LoBind resulted in the most significant loss of all containers

tested. PS resulted in less loss than PP for 44AHJD and P68 but was worse than PP when used to store gh-1. Similar to the result obtained with PP, incubation of PS with BSA appears to improve retention by between 1 and 1.8 $\log_{10}$ relative to untreated PS. The IT of 44AHJD decreased significantly more slowly in containers other than glass, where very rapid decay was observed. In the case of P68, IT drops homogenously and most rapidly in glass, PS and BSA-treated containers in the first two days before stabilizing. However, the titer of P68 stored in PP and PP LoBind did not stabilize, even after two weeks of storage. In contrast, the IT of gh-1 evolves more slowly than P68 but comparably to 44AHJD. In PP and PS treated with BSA, the titer remained stable at approximately the initial titer (less than 0.22 $\log_{10}$ loss) for the duration of the experiment. After an initial loss of IT, by day 14 phage P68 exhibited a rebound of 1.13 $\log_{10}$ in PS+BSA and 0.9 $\log_{10}$ PP+BSA compared to their value after one day in storage.

The Kruskal-Wallis H test revealed that the resulting infectious titer loss was statistically different, depending on the storage container, with H= 47.5, 33.1, and 33.1 for 44AHJD, P68, and gh-1, respectively; the p-value was less than 0.001 for all three phages.

Infectious titer determination for three separate phages in six different containers involves a significant overhead in terms of both laboratory waste and manual counting to be performed. Despite the economies afforded by the drop-cast method used (Chhibber *et al.*, 2018) over the double layer agar method (Adams, 1959), approximately 15,000 individual plaques were counted from 2,500 individual drop cast assays. In order to limit the waste produced and increase the statistical significance of the results of plaque counting experiments, a strategic guess was made at each timepoint regarding the likely infectious titer, and in most cases three or four dilutions were plated rather than the full set of ten serial dilutions. For example, the 10^{-1} to 10^{-4} dilutions contain far too many plaques to be countable, and the higher dilutions from 10^{-9} to 10^{-10} were too dilute for P68 and gh-1 to produce even a single lysis plaque. Plating more replicates of a selection of dilutions permitted 16 drop cast assays in each petri dish, typically with between four and six replicates of each dilution per dish.

Following observation of IT loss in plaque counting experiments, it was hypothesized that this loss could be due to some combination of inactivation, aggregation, and/or adsorption on the container walls. In order to compare the infectious titer with the aggregation state and particle concentrations of phage suspensions following storage, particle size distributions were produced by nanoparticle tracking analysis (NTA). NTA involves the tracking of individual nanoparticles in order to analyse their Brownian motion and evaluate their volume concentration (Kramberger *et al.*, 2012). From the observed motion of the particles, the diffusion coefficient and hence hydrodynamic radius can be inferred. NTA was performed at the end of the experimental sequence for all three phages in all six container types (18 suspensions total, Figure 2). NTA produced size distributions that indicate a very high level of aggregation of 44AHJD and P68 suspensions stored in glass, and intermediate aggregation of P68 and gh-1 in PP LoBind containers, as indicated by heavily skewed distributions and large increases in the mean and median particle size relative to other containers (Figure 2). BSA-treatment of PP and PS containers yields distributions with consistently smaller particle size for all phages except 44AHJD in PP+BSA, where moderate broadening of the distribution was observed. Suspensions of gh-1 stored in PP and PP+BSA showed the highest monodispersity of all samples. Infectious titer of gh-1 stored in PS was too low for NTA measurement, which requires at least 10^7 particles ml^{-1}. Plotting 90^{th} percentile particle diameter (P_{90}) against infectious titer loss after two weeks in storage (Figure 3), a correlation between aggregation and IT loss is revealed — driven particularly by glass containers — with a power law fit yielding an R^2 value of 74 %. However, inclusion of total particle concentration paints a more intricate picture of IT loss.

A distinction must be made between infectious titer and the concentration of viral particles in a phage suspension. The infectious titer is a measure of the presumed viral load of a parent suspension, as calculated from the observed count of lysis plaques produced in plaque-counting methods, together with the dilution factor of the plated sample. Plaque-counting methods are incapable of detecting empty phages or distinguishing between a single phage and aggregates of multiple phage particles. In contrast, nanoparticle tracking analysis reveals the hydrodynamic radius and optical scattering properties of individual particles, with little discrimination between viable phages, empty phages, phage aggregates, or contaminants.

In this work, both adsorption, aggregation, and inactivation are likely to occur in parallel, with the balance between these phenomena varying based on container material. We propose a model by which tandem plaque counting and NTA measurements can be interpreted to reveal the nature of infectious titer loss, as shown in Figure 4. Depending on three variables — infectious titer (PFU ml^{-1}), particle concentration (PC; particles ml^{-1}), and aggregation state (P_{90})— we can make inferences about the causes of IT decay. Log_{10} discrepancies in the ratio of infectious titer to total particle concentration are shown by diagonal contours. For example, a datapoint at the 10^{-3} contour indicates a suspension in which a small minority of only one in 10^3 particles is infectious. Pure phage aggregation should result in the same number of lysis plaques being produced as the number of particles detected in NTA, since each particle aggregate will initiate a single lysis plaque despite being composed of multiple phage particles. Such aggregation — in the absence of phage inactivation — produces a data point along the identity line in the PC/IT plots of Figure 4. Phage adsorption to container walls will similarly yield a datapoint along the identity line since the ratio of infectious to total particles in the bulk remains the same. In order to disambiguate between adsorption and aggregation, we must consider the particle size distribution which is also measured by NTA. Datapoint diameters in Figure 4 have been scaled to correspond to the 90^{th} percentile particle diameter (P_{90}; nm) for each suspension. P_{90} is a more reasonable proximal measure for phage aggregation than mean or median diameter, since this value takes into account the disproportionate contribution of large aggregates to titer loss (a single 500 nm aggregate could contain hundreds of phages). Datapoints near the identity line in Figure 4 can be interpreted as indicating aggregation if they feature a large P_{90}, or adsorption if they feature a small P_{90}, since in both cases they result in a reduction of PC commensurate with reduction in IT. In contrast, pure phage inactivation manifests as a decrease in the infectious titer that is independent of the number of particles measured by NTA, since inactivated phages are still observable by NTA. Inactivation is thus indicated by vertically downward movement in the PC/IT plot.

Finally, it should be pointed out that if the P_{90} increases significantly (indicating aggregation) then datapoints become ambiguous because of two effects. Firstly, aggregation will mask adsorption since both phenomena reduce the PC and IT proportionately (diagonal movement along contour). Secondly, aggregation will mask inactivation, since it is not possible to observe if a lysis plaque is initiated by a

single phage or multiple phages within an aggregate. For this reason, there remains some ambiguity in the contribution of inactivation and adsorption when large P_{90} datapoints occur, which necessitates analysis by other means (*e.g.,* SEM of container surfaces to ascertain level of adsorption).

The PC/IT plot for 44AHJD shows an almost vertical alignment of data points for all containers, with low levels of aggregation for all containers except glass. The close lateral clustering of all 44AHJD datapoints around $\sim 10^{11}$ particles mL^{-1} suggests that IT loss was mainly driven by inactivation in polymer containers, with the exception of glass containers where a large P_{90} value indicated a strong contribution of aggregation in glass. Adsorption appeared to be less of a driver of IT loss of 44AHJD compared to other phages, which is consistent with the existence of a saturation density on the container surface (Richter *et al.*, 2021) that is quickly satisfied for 44AHJD which was the highest-titer suspension. Finally, blocking PP and PS surfaces with BSA resulted in datapoints nearest the top right of the PC/IT plot for 44AHJD, indicating a reduction of both inactivation and adsorption, consistent with a blocking of interaction with the polymer surface by a BSA adlayer.

In contrast, several insights allow us to infer that a combination of adsorption and inactivation dominated during storage of P68 and gh-1 in polymer (PP, PS, and PP LoBind) containers. Firstly, pure adsorption results in datapoints along the identity line of the PC/IT plot, which is what was observed for gh-1 stored in PP.

Movement towards the bottom-left of PC/IT plots — if not accompanied by an increase in P_{90} — indicates a combination of adsorption and inactivation, since the total particle number (both infective and not) is decreasing (diagonal movement along contour), and also the fraction of particles that are infective is decreasing (vertical downward movement). This combination of adsorption and inactivation was observed for P68 and gh-1 stored in PP LoBind.

As observed with 44AHJD suspensions, storage in glass appears to have a very different effect on P68 and gh-1 compared to storage in polymer containers. This is indicated by the position of glass-stored datapoints towards the right-hand side of PC/IT plots of gh-1 and P68. While a small P_{90} indicates inactivation of gh-1 in glass, a larger P_{90} indicates significant aggregation of P68.

While NTA analysis yielded peaks of 36-56 nm for 44AHJD and 32-62 nm for P68, respectively (Figure 2) both phages are quoted in the literature as having a 75 nm isometric head (Vybiral *et al.*, 2003). A possible explanation for this discrepancy is that the NTA software assumes a spherical particle in its calculation of the diameter (*NanoSight NTA 2.1 Analytical Software Operating Manual*, 2010). Departure of phage geometry from an ideal sphere may account for the difference in diameter between the literature and observed in this work by NTA.

Following NTA measurements, it was hypothesized that glass was preferentially inducing both aggregation and inactivation, while PP was mainly leading to inactivation with some absorption, and PP+BSA was merely slightly adsorbing phage. In order to investigate the level of phage adsorption on container surfaces, SEM analysis was performed on the inner surfaces of glass, polypropylene, and BSA-treated polypropylene containers that had been used to store phage 44AHJD (Figure 5). These surfaces were selected since analysis of all containers would be impractical, yet these three surfaces should elucidate the mechanisms underlying infectious titer loss and validate our interpretation of PC/IT plots. All glass and untreated PP surfaces observed were shown to be free of particles resembling phages. In the case of PP+BSA, however, adsorbed phage-like particles were observed with a density of 0.44 ± 0.08 phage μm^{-2}. The observed titer loss from the suspension stored in this container, if due entirely to adsorption, should result in phages present on the container walls with a surface density of between 0.1-2 phage μm^{-2}, which agrees with our interpretation of the PC/IT plots that IT loss of this suspension in this container is driven by absorption, since the data point is found near the identity line with a small P_{90} value. Increased surface roughness was observed on PP+BSA surfaces, intermediate roughness on PP, and very low roughness on glass.

Recent publications posited a correlation between wettability of labware material and modulation of stability of phage suspensions stored in them (Richter *et al.*, 2021; Wdowiak *et al.*, 2021). Richter *et al.* found that an increase in container surface contact angle resulted in a transition to instability above a threshold of 95°, which the authors propose as a heuristic to approximately judge suitability of labware for phage storage. In an attempt to replicate these results for the containers in this study, and furthermore to investigate if the same correlation holds for BSA-treated surfaces, contact angle

measurements were carried out on identically prepared containers to those used to store phage suspensions. The results of water contact angle measurements are summarized in Table S2. Immobilization of BSA on the PP and PS layers is partly confirmed by the observed modification of the surface wetting properties of these surfaces relative to their untreated forms. Incubating PS and PP tubes with BSA overnight was shown to result in an increase in the hydrophilic character of these materials and thus a decrease in the contact angle in each case (decrease of -25.2° for PP and -35.4° for PS). Furthermore, BSA treatment seems to bring both the PP and PS hydrophilicity to a similar level, as evidenced by the fact that they exhibit more similar contact angles after treatment (difference of 4.8°), than beforehand (difference of 15°).

Phage 44AHJD appears to show good stability for PP+BSA, PS+BSA, and PP LoBind —materials whose contact angles are clustered in the range (59.3-64.1°). 44AHJD was the only phage to experience an increase in stability when stored in PP LoBind. In comparison, P68 and gh-1 experienced over 3 $\log_{10}$ more IT loss in PP LoBind tubes. Plotting the contact angle against the drop in infectious titer, we see no clear correlation between contact angle and phage stability (Figure 6). We also see that BSA-treated surfaces result in a very similar level of titer decay, regardless of the underlying polymer. While PP containers result in significantly different levels of IT loss depending on phage, the loss in PP+BSA and PS+BSA is more clustered compared to all other containers.

Discussion

NTA and plaque counting form complementary, tandem measurements, which together reveal richer insights into the evolution of the phage suspension titer and aggregation state, compared to either technique alone. NTA yields individual particle information across statistically significant sample sizes (Malvern, 2017) and has been demonstrated for the study of bacteriophage (Hsiao *et al.*, 2016; Kaletta *et al.*, 2020) and viral suspensions (Du *et al.*, 2010; Szakács *et al.*, 2018). In contrast, dynamic light scattering (DLS) yields ensemble averages of diffusion coefficients (and extrapolated distributions of hydrodynamic radius). While DLS is an established technique for analysis of nanoparticle dispersions, it can struggle to give interpretable results for suspensions with significant polydispersity. NTA thus

presents advantages over DLS in the study of bacteriophage suspensions, particularly in cases where aggregation is suspected, and yields more granular data.

A naïve interpretation of the drop cast plaque assay would show a simple reduction in infectious titer, obscuring the root cause. Complementing plaque counting measurements with NTA and SEM reveals that the causes of IT decay are manifold, with contributions from aggregation, inactivation, and adsorption depending on container material, with aggregation particularly severe in the case of glass containers. Storage in glass and PP LoBind containers resulted in the most dramatic reduction in IT, and in the case of glass correlated with a skew towards larger particle diameter. In the case of untreated PP, PS, and PP LoBind, the reduction in titer was not commensurate with increased aggregation and so is more likely attributable to inactivation of phages or adsorption on container walls. For instance, in the case of P68 in PP LoBind, only one particle in 10^4 is still infectious after two weeks, while P_{90} is low , highlighting the major role of inactivation. Our results demonstrate the value of NTA as a complementary measurement to traditional plaque assays to interrogate aggregation state of phage suspensions. Without such information, one is essentially "flying blind" when drawing conclusions from plaque counting methods, with regards to the nature of infectious titer loss.

Recent work by Richter *et al.* has shown that choice of container material is an important determinant of stability of bacteriophage suspensions in storage (Richter *et al.*, 2021). Inspired by this result, we attempted to replicate the same results with three phages of a different morphology. While Richter *et al.* observed a strong correlation between contact angle and titer loss, we have observed no clear correlation between contact angle and IT decay across a variety of container material and surface treatments. We observed dramatic titer loss in polypropylene containers, which has been shown to be a consistently unsuitable material with regards to phage stability (Duyvejonck *et al.*, 2021; Richter *et al.*, 2021; Wdowiak *et al.*, 2021). Contrary to our expectations, substituting standard polypropylene with low protein-binding formulations exacerbated the problem, resulting in IT loss of 4.65 and 4.22 $\log_{10}$ loss of phages P68 and gh-1, respectively. In fact, IT in PP LoBind containers did not stabilize even by the end of the two-week experiment, and so IT loss is likely to progress further following storage for longer durations. In contrast, the observed retention of IT in the case of phage 44AHJD in

PP LoBind containers indicates that choice of container material must be tailored to each phage and that contact angle is not a consistent determinant of phage stability. We also observed significant and the most rapid IT loss in glass containers, in contradiction to previous research wherein storage in glass was observed to result in almost no detectable drop in infectious titer (Richter *et al.*, 2021). However, the work of Richter *et al.* examined only phage T4, a myovirus with very different morphology to the three podoviruses presented in this work, which could explain these divergent observations since phage morphology can be a determinant of stability (Lytle *et al.*, 1991). Furthermore, our results replicate the findings of Lytle *et al.* who also demonstrated loss of IT following exposure to glass, although the authors were unable to reveal the nature of the observed IT loss.

Instead of a correlation between contact angle and IT decay, we instead saw a correlation between surface roughness and IT loss, as detailed below. SEM analysis of container interior surfaces allowed us to investigate the role of surface adsorption in IT loss of phage 44AHJD in glass, PP and PP+BSA containers. The observed titer loss from the suspension, if due entirely to adsorption, should result in phage present on these container walls with a surface density of between 0.1-2 phage μm^{-2}. In the case of PP+BSA, adsorbed particles were indeed observed with a density of 0.44 ± 0.08 phage μm^{-2}, validating our interpretation of IT/PC plots as indicating that adsorption dominates in these containers. Particles resembling phage were not found on the surfaces of glass or PP containers, which implies that phage were either inhomogeneously deposited on the surface with a very high concentration in regions other than those observed by SEM, or that adsorption is not a significant contributor to IT decay.

Previous studies show that inactivation of phages in suspension is related to the available surface area of the air-water interface, where extrusion of the phage capsid hydrophobic domains into the air phase causes the proteins to denature (Trouwborst *et al.*, 1974). Interaction with this interface is insufficient to explain the difference in phage titer loss in our work, however, since the ratio of the liquid phase volume to air-water interface area was very similar between glass and polypropylene containers despite large differences in IT decay rate. Thompson and Yates observed the same inactivation of

phage in polypropylene containers as in our work (Thompson and Yates, 1999) but attributed inactivation not to the air-water interface but rather to the triple-phase-boundary (TPB) where air, liquid, and container tube wall phases intersect (Thompson *et al.*, 1998). However, this inactivation effect depends on a hydrophobic tube wall, which is not the case in our glass and PP LoBind containers, which also exhibited the worst phage stability. Furthermore, we observed no correlation between IT loss and the ratio of the length of the TPB to volume (L_{TPB}/V), as proposed by (Thompson and Yates, 1999). Since no significant deposits of phage were found on glass and PP surfaces, we consider aggregation or inactivation to be more likely explanations for the observed reduction in IT in containers other than PP+BSA. This leaves two possibilities: either contact with the surface directly induces inactivation and/or aggregation, or material leaches from the surface to induce the same effects in the bulk.

If material leaches into the bulk from the container material and causes phage aggregation/inactivation, the same should be true in the case of BSA-treated containers. Furthermore, Richter *et al.* effectively excluded the possibility of leachables as a major contributor to IT decay in their own containers (Richter *et al.*, 2021), and we do not consider this to be a plausible explanation in our work either since any leachables should still be able to diffuse through an adsorbed BSA layer and induce IT loss, which was not observed. Finally, glass containers — which resulted in some of the worst IT loss — are not expected to be capable of releasing material into the bulk. This leaves contact interactions between phage and the surface itself as the most likely explanation of IT decay that was observed in this work.

With the potential explanations of adsorption, interactions with the air-water interface and/or triple-phase-boundaries, and no correlation with hydrophobicity of the container walls, we hypothesize that an additional causative factor of IT loss is container surface nanotopography. Nanoscale surface topography has been found to modulate aggregation of various proteins including amyloid-β peptides on polystyrene (Shezad *et al.*, 2016) and amylin on silicon oxide (Hanke *et al.*, 2021), with increasing surface smoothness correlated with more rapid aggregation. Co and Li recently provided a model for understanding this phenomenon, showing in Monte Carlo simulations that an increase in roughness

slows amyloid fibril formation (Co and Li, 2021). Kam *et al.* have found that nanotopography of polystyrene and polypropylene was a greater determinant of water contact angle than chemical composition (Kam *et al.*, 2014), while Nie *et al.* observed that the increase in wettability of plasma-treated polypropylene is coincident with a change to smoother surface topography (Nie *et al.*, 1999). Our SEM analysis of glass, PP and PP+BSA containers revealed the surface topography of glass to be significantly smoother than that of PP and PP+BSA. This indicates a correlation between increasing surface roughness and increasing phage stability in our experiments. Our findings are consistent with the observed modulation of aggregation by surface nanotopography that has been established in the literature for proteins, but should be compared with an observation of the opposite effect for bacteriophages of a different myovirus morphology (Dika *et al.*, 2013). While the work of Dika *et al.* showed the lowest level of adhesion on glass surfaces, the study did not control for surface material while varying roughness, and furthermore did not observe a monotonic correlation between roughness and phage adhesion. In any case, we do not attribute IT loss in glass containers to adhesion but rather to aggregation. For these reasons we do not find the findings of Dika *et al.* to be incompatible with our hypothesis of a correlation between roughness and aggregation.

Richter *et al.* found that plasma treatment of polypropylene containers reduced IT decay, attributing this to an increased hydrophilicity of the surface. However, such an explanation is in contradiction both to our work and to the findings of Wang *et al.* who observed almost no adsorption of T4 phage on polyhydroxyalkanoate surfaces with a wetting angle of 96.83°, but *increased* adsorption following plasma-treatment and an associated decrease in the contact angle to 14.96° (Wang *et al.*, 2016). This latter result is more consistent with our own observation of significant IT decay in glass vials which had a contact angle of 13.6°. Further supporting a hypothesis of nanotopographical modulation of phage stability, Wdowiak *et al.* demonstrated that coating of container surfaces with gold—polyoxoborate nanocomposites prevented adsorption of phages on polypropylene labware (Wdowiak *et al.*, 2021). As in the earlier work of Richter *et al.* this protective effect was similarly attributed to modification of the wettability. However, the proposed nanocomposite treatment also significantly altered the nanotopography of the polypropylene surface, and the authors report an increasing phage

protection effect with increasing deposition, and presumably a commensurate increase in surface roughness.

We propose that both water contact angle and nanotopography have an influence on phage aggregation. Indeed, Richter *et al.* show that the "safe" tubes seem to be those whose surface topography exhibited the highest spatial frequency, as revealed by AFM analysis (Richter *et al.*, 2021). Furthermore, that paper showed that increased mixing and higher temperature had the effect of increasing IT decay. It is possible that this increase was due to increased lateral diffusion of phage on the container walls, which is normally impeded by nanoscale roughness (and thus leads to slower IT decay) which can be overcome by agitation and thermal motion and result in the formation of aggregates which either remain on the surface or migrate back to the bulk (Rabe *et al.*, 2011). A nanotopography dependence of IT loss is consistent with our own observations, since untreated PP was observed to have a higher nanoscale roughness than glass, resulting in IT decay that was *delayed* relative to glass but continued even after two weeks of storage, while PP+BSA was observed to have the highest roughness and lowest IT loss.

One of the most striking results from phage enumeration experiments was the improvement in infectious titer retention after treatment of PP and PS labware with BSA. This supports the hypothesis that pre-saturating the surface with protein can protect against loss of infectious titer. Our findings can be compared with those of Lytle *et al.*, who found that inclusion of calf serum in phage suspensions prevented IT loss of several podovirus phages following exposure to vinyl, latex and glass (Lytle *et al.*, 1991) and reduced adhesion to nitrocellulose and polysulfone membranes (Lytle and Routson, 1995). Although calf serum is a more complex additive than pure bovine serum albumin, both our work and that of Lytle *et al.* show a protective effect when protein is allowed to adhere to labware surfaces. Rossi et al. found that addition of BSA to a phage suspension can induce an increase in infectious titer as BSA displaces phage adsorbed on clay particulate surfaces (Rossi and Aragno, 1999). A similar effect may explain the increase of IT after an initial decrease in the case of phage P68 stored in PP+BSA and PS+BSA containers. Our findings indicate that incubating protein with the surface is sufficient to impede phage loss, negating the necessity to add protectant directly to the phage suspension, which

could have important implications for pharmaceutical compatibility of phage preparations. It is possible that BSA remains loosely bound to the container surface and subsequently leaches back into the suspension, either interacting with phages themselves in such a way that prevents infectious titer loss, or perhaps migrating to the air-water interface to block free phage from interacting with the air phase (Thompson and Yates, 1999). However, all BSA-treated containers were thoroughly rinsed several times before introduction of phage, and were not subsequently exposed to detergent, heat or changes in salinity or pH which may lead to solubility or conformational changes that could cause BSA to desorb. We conclude, then, that the protective effect of BSA may rely on reducing contact between phage and the bare container surface. Further work is necessary to establish the level of BSA leaching from the surface back into the bulk in order to elucidate the nature of the protective effect of BSA.

In this work, we have shown that phage infectious titer drops rapidly in common labware, partly replicating results recently presented in the literature, but finding that storage in glass and low-binding polypropylene labware induced the most rapid and drastic loss of infectious titer of phage suspensions. We propose that several phenomena — adsorption, aggregation, and inactivation — are at play simultaneously, and that the balance between them depends on the nanotopography and/or material composition of the container surface, supporting this hypothesis with comparison between infectious titer and particle size distributions generated by NTA.

NTA was demonstrated as a valuable, complementary measure of the total particle concentration and aggregation state of phage suspensions, revealing the multifaceted nature of infectious titer loss. Water contact angle measurements of container interior surfaces did not yield a correlation between wettability and phage titer stability for any of the three phages studied, contradicting recently published results. Further work is needed to correlate a full characterization of container material surface energy (*i.e.*, more thorough than only the sessile drop method with deionized water) with infectious titer loss of exposed phage suspensions.

Pre-incubation of container surfaces with bovine serum albumin was demonstrated as a simple and effective method to significantly reduce infectious titer loss. Scanning electron microscopy was performed on container surfaces in order to assess the level of phage surface adsorption, suggesting

that adsorption accounts for infectious titer decay in PP+BSA containers, while aggregation and inactivation were more important determinants of phage stability in glass and polypropylene containers.

The observed loss of infectious titer has important implications for fundamental research on phage and their use in biomedical applications. Further investigation into the modulation of infectious titer loss by container material and surface topography could yield phage-optimized storage protocols and contribute to consistency and repeatability in phage research.

Acknowledgments

The *Félix d'Hérelle Reference Center for Bacterial Viruses* at the Université Laval (Québec, Canada) is gratefully acknowledged for providing gh-1, 44AHJD and P68 bacteriophages, as well as bacterial host strain *Pseudomonas putida* ATCC 12633.

The authors would also like to thank:

Christine Chatellard at the Institut de Biologie Structurale, Grenoble, for assistance with NTA measurements.

Amelia Whiteley, for contact angle measurements.

Pierre-Henri Jouneau at CEA-Leti for assistance with electron microscopy.

This work has been partially supported by Labex ARCANE and CBH-EUR-GS (Grant ANR-17-EURE-0003).

References

Adams, M.H. (1959) *Bacteriophages*. New York: Interscience Publishers.

Bechtold, B. (2016) 'Violin Plots for Matlab, Github Project'. doi:10.5281/zenodo.4559847.

Biswas, B. *et al.* (2018) 'Phage Therapy for a Multidrug-Resistant Acinetobacter baumannii Craniectomy Site Infection', *Open Forum Infect. Dis.*, 5(4), pp. 1–3. doi:10.1093/ofid/ofy064.

Chhibber, S. *et al.* (2018) 'Simple drop cast method for enumeration of bacteriophages', *J. Virol. Methods*, 262(August), pp. 1–5. doi:10.1016/j.jviromet.2018.09.001.

Co, N.T. and Li, M.S. (2021) 'Effect of surface roughness on aggregation of polypeptide chains: A monte carlo study', *Biomolecules*, 11(4), pp. 1–16. doi:10.3390/biom11040596.

Dika, C. *et al.* (2013) 'Non-DLVO adhesion of F-specific RNA bacteriophages to abiotic surfaces: Importance of surface roughness, hydrophobic and electrostatic interactions', *Colloids Surfaces A Physicochem. Eng. Asp.*, 435, pp. 178–187. doi:10.1016/j.colsurfa.2013.02.045.

Du, S. *et al.* (2010) 'Measuring number-concentrations of nanoparticles and viruses in liquids on-line', *J. Chem. Technol. Biotechnol.*, 85(9), pp. 1223–1228. doi:10.1002/jctb.2421.

Duyvejonck, H. *et al.* (2021) 'Evaluation of the stability of bacteriophages in different solutions suitable for the production of magistral preparations in Belgium', *Viruses*, 13(5), pp. 1–11. doi:10.3390/v13050865.

Fedorenko, A. *et al.* (2020) 'Survival of the enveloped bacteriophage Phi6 (a surrogate for SARS-CoV-2) in evaporated saliva microdroplets deposited on glass surfaces', *Sci. Rep.*, 10(1), p. 22419. doi:10.1038/s41598-020-79625-z.

Ferry, T. *et al.* (2018) 'Salvage debridement, antibiotics and implant retention ("DAIR") with local injection of a selected cocktail of bacteriophages: Is it an option for an elderly patient with relapsing staphylococcus aureus prosthetic-joint infection?', *Open Forum Infect. Dis.*, 5(11), pp. 1–4. doi:10.1093/ofid/ofy269.

Hanke, M. *et al.* (2021) 'Nanoscale surface topography modulates hiapp aggregation pathways at solid–liquid interfaces', *Int. J. Mol. Sci.*, 22(10). doi:10.3390/ijms22105142.

Hintze, J.L. and Nelson, R.D. (1998) 'Violin Plots: A Box Plot-Density Trace Synergism', *Am. Stat.*, 52(2), pp. 181–184. doi:10.1080/00031305.1998.10480559.

Howes, D.W. (1969) 'Overlap and the Errors of Plaque Counting I. The Overlap Biases of Observed Counts and their Correction', *J. Hyg. (Lond).*, 67(2), pp. 317–334. doi:10.1017/S0022172400041723.

Howes, D.W. and Fazekas de St Groth, S. (1969) 'Overlap and the Errors of Plaque Counting II. The Bias of the Variance and the Concealment of Errors', *J. Hyg. (Lond).*, 67(2), pp. 335–342. doi:10.1017/S0022172400041735.

Hsiao, Y.H. *et al.* (2016) 'Continuous microfluidic assortment of interactive ligands (CMAIL)', *Sci. Rep.*, 6(May), pp. 1–11. doi:10.1038/srep32454.

Hu, J.Y. *et al.* (2003) 'Removal of MS2 bacteriophage using membrane technologies.', *Water Sci. Technol. a J. Int. Assoc. Water Pollut. Res.*, 47(12), pp. 163–168.

Jault, P. *et al.* (2018) 'Efficacy and tolerability of a cocktail of bacteriophages to treat burn wounds infected by Pseudomonas aeruginosa (PhagoBurn): a randomised, controlled, double-blind phase 1/2 trial', *Lancet Infect. Dis.*, 3099(18), pp. 1–11. doi:10.1016/S1473-3099(18)30482-1.

Kakasis, A. and Panitsa, G. (2019) 'Bacteriophage therapy as an alternative treatment for human infections. A comprehensive review', *Int. J. Antimicrob. Agents*, 53(1), pp. 16–21. doi:10.1016/j.ijantimicag.2018.09.004.

Kaletta, J. *et al.* (2020) 'A rigorous assessment and comparison of enumeration methods for environmental viruses', *Sci. Rep.*, 10(1), pp. 1–12. doi:10.1038/s41598-020-75490-y.

Kam, K.R. *et al.* (2014) 'The effect of nanotopography on modulating protein adsorption and the fibrotic response', *Tissue Eng. - Part A*, 20(1–2), pp. 130–138. doi:10.1089/ten.tea.2012.0772.

Kramberger, P. *et al.* (2012) 'Evaluation of nanoparticle tracking analysis for total virus particle determination', *Virol. J.*, 9, pp. 1–10. doi:10.1186/1743-422X-9-265.

Langlet, J. *et al.* (2008) 'Aggregation and surface properties of F-specific RNA phages: Implication for membrane filtration processes', *Water Res.*, 42(10–11), pp. 2769–2777. doi:10.1016/j.watres.2008.02.007.

Lee, L.F. and Boezi, J.A. (1966) 'Characterization of bacteriophage gh-1 for Pseudomonas putida.', *J. Bacteriol.*, 92(6), pp. 1821–1827.

Lytle, C.D. *et al.* (1991) 'Important factors for testing barrier materials with surrogate viruses', *Appl. Environ. Microbiol.*, 57(9), pp. 2549–2554. doi:10.1128/aem.57.9.2549-2554.1991.

Lytle, C.D. and Routson, L.B. (1995) 'Minimized virus binding for tests of barrier materials', *Appl. Environ. Microbiol.*, 61(2), pp. 643–649. doi:10.1128/aem.61.2.643-649.1995.

Malvern (2017) *Viruses and Viral Vaccines : Characterization by Nanoparticle Tracking Analysis*.

NanoSight NTA 2.1 Analytical Software Operating Manual (2010). NanoSight Ltd.

Nie, H.Y. *et al.* (1999) 'Atomic force microscopy study of polypropylene surfaces treated by UV and ozone exposure: Modification of morphology and adhesion force', *Appl. Surf. Sci.*, 144–145, pp. 627–632. doi:10.1016/S0169-4332(98)00879-4.

O'Connell, L. *et al.* (2021) 'Strategies for Surface Immobilization of Whole Bacteriophages: A Review', *ACS Biomater. Sci. Eng.*, 7(6), pp. 1987–2014. doi:10.1021/acsbiomaterials.1c00013.

Perlemoine, P. *et al.* (2021) 'Phage susceptibility testing and infectious titer determination through wide-field lensless monitoring of phage plaque growth', *PLoS One*, 16(3 March), pp. 1–14. doi:10.1371/journal.pone.0248917.

Rabe, M. *et al.* (2011) 'Understanding protein adsorption phenomena at solid surfaces', *Adv. Colloid Interface Sci.*, 162(1–2), pp. 87–106. doi:10.1016/j.cis.2010.12.007.

Richter, Ł. *et al.* (2021) 'Adsorption of bacteriophages on polypropylene labware affects reproducibility of phage research', *Sci. Rep.*, 11(7387). doi:10.1038/s41598-021-86571-x.

Rosenblum, E.D. and Tyrone, S. (1964) 'Serology, Density, and Morphology of Staphylococcal Phages', *J. Bacteriol.*, 88(6), pp. 1737–1742. doi:10.1128/jb.88.6.1737-1742.1964.

Rossi, P. and Aragno, M. (1999) 'Analysis of bacteriophage inactivation and its attenuation by adsorption onto colloidal particles by batch agitation techniques', *Can. J. Microbiol.*, 45(1), pp. 9–17. doi:10.1139/cjm-45-1-9.

Schindelin, J. *et al.* (2012) 'Fiji: an open-source platform for biological-image analysis', *Nat. Methods*, 9(7), pp. 676–682. doi:10.1038/nmeth.2019.

Shezad, K. *et al.* (2016) 'Surface Roughness Modulates Diffusion and Fibrillation of Amyloid-β Peptide', *Langmuir*, 32(32), pp. 8238–8244. doi:10.1021/acs.langmuir.6b01756.

Staquicini, D.I. *et al.* (2021) 'Design and proof of concept for targeted phage-based COVID-19 vaccination strategies with a streamlined cold-free supply chain', *PNAS*, 118(30). doi:10.1073/pnas.2105739118.

Szakács, Z. *et al.* (2018) 'Selective counting and sizing of single virus particles using fluorescent aptamer-based nanoparticle tracking analysis', *Nanoscale*, 10, pp. 13942–13948. doi:10.1039/c8nr01310a.

Thompson, S.S. *et al.* (1998) 'Role of the Air-Water-Solid Interface in Bacteriophage Sorption Experiments', *Appl. Environ. Microbiol.*, 64(1), pp. 304–309. doi:10.1128/aem.64.1.304-309.1998.

Thompson, S.S. and Yates, M. V. (1999) 'Bacteriophage inactivation at the air-water-solid interface in dynamic batch systems', *Appl. Environ. Microbiol.*, 65(3), pp. 1186–1190. doi:10.1128/aem.65.3.1186-1190.1999.

Trouwborst, T. *et al.* (1974) 'Inactivation of some bacterial and animal viruses by exposure to liquid air interfaces', *J. Gen. Virol.*, 24(1), pp. 155–165. doi:10.1099/0022-1317-24-1-155.

Vybiral, D. *et al.* (2003) 'Complete nucleotide sequence and molecular characterization of two lytic Staphylococcus aureus phages: 44AHJD and P68', *FEMS Microbiol. Lett.*, 219(2), pp. 275–283.

doi:10.1016/S0378-1097(03)00028-4.

Wang, C. *et al.* (2016) 'Immobilization of Active Bacteriophages on Polyhydroxyalkanoate Surfaces', *ACS Appl. Mater. Interfaces*, 8(2), pp. 1128–1138. doi:10.1021/acsami.5b08664.

Wdowiak, M. *et al.* (2021) 'Gold—polyoxoborates nanocomposite prohibits adsorption of bacteriophages on inner surfaces of polypropylene labware and protects samples from bacterial and yeast infections', *Viruses*, 13(7). doi:10.3390/v13071206.

Wright, A. *et al.* (2009) 'A controlled clinical trial of a therapeutic bacteriophage preparation in chronic otitis due to antibiotic-resistant Pseudomonas aeruginosa ; a preliminary report of efficacy', *Clin. Otolaryngol.*, 34, pp. 349–357. doi:10.1111/j.1749-4486.2009.01973.x.

Figures

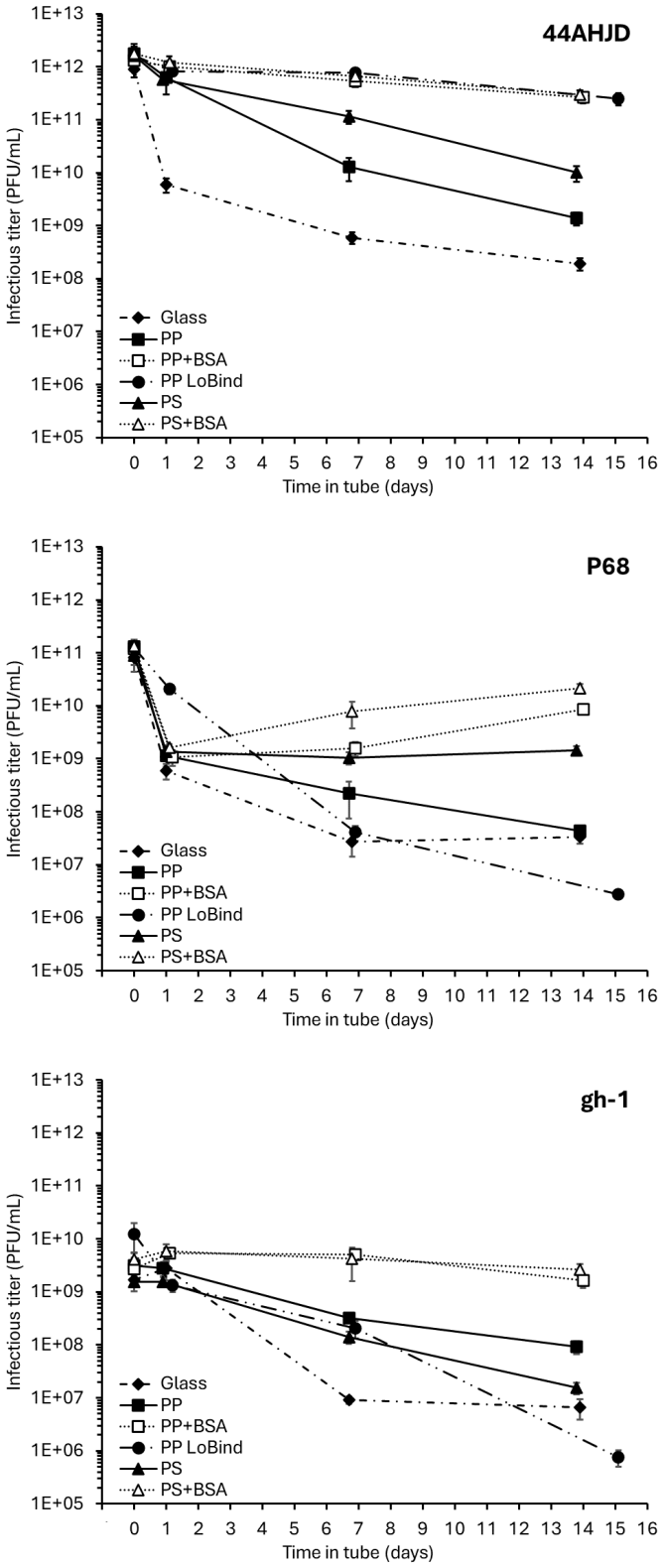

Figure 1 Semi-log plots of decay of infectious titer for bacteriophages 44AHJD (top), P68 (centre), and gh-1 (bottom); after storage for various durations at 4 °C in glass (◆), polypropylene (■), BSA-treated polypropylene

(□), low-binding polypropylene (●), polystyrene (▲), and BSA-treated polystyrene (△) containers. Each data point reflects between 4-16 replicates of a single phage-container pair. Error bars indicate the experimental uncertainty as discussed in the Supporting Information. For clarity, the infectious titer at day 2 is not shown, but can be found in the Supporting Information Table S2.

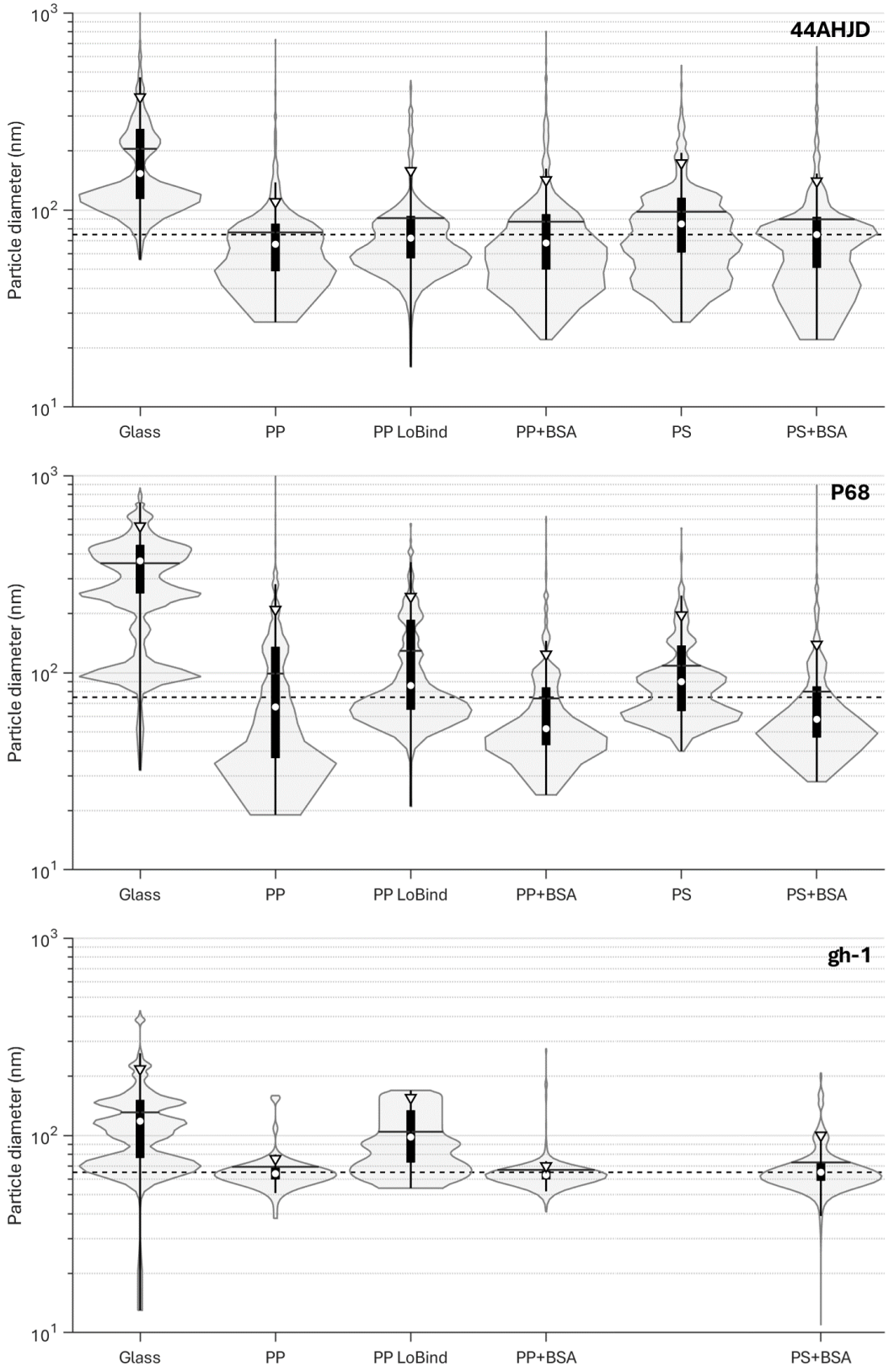

Figure 2 Semi-log violin plots of particle size distributions obtained by nanoparticle tracking analysis (NTA) of suspensions of 44AHJD (top), P68 (centre), and gh-1 (bottom); following two weeks of storage in each container.

The width of each plot indicates the relative proportion of particles of that diameter within each distribution respectively. The median (○), mean (solid horizontal bars), and P_{90} (▽) are indicated in each distribution. Dashed horizontal line indicates the capsid diameters as determined for 44AHJD and P68 by Vybiral et al. (2003); and for gh-1 by transmission electron microscopy.

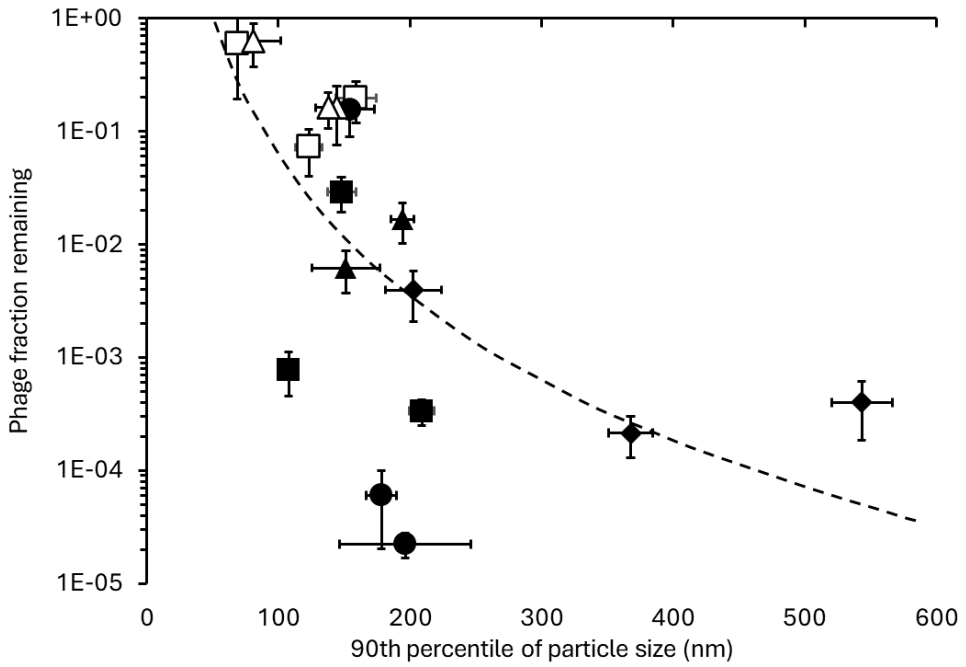

Figure 3 Semi-log scatter plot of 90th percentile of particle diameter (as observed by nanoparticle tracking analysis) vs. remaining fraction of initial infectious titer (as measured by plaque counting) after storage for two weeks in glass (◆), polypropylene (■), BSA-treated polypropylene (□), low-binding polypropylene (●), polystyrene (▲), and BSA-treated polystyrene (△) containers. A power law fit (R^2=74%) is indicated with a dashed line. Error bars in the x-direction indicate the standard deviation of P_{90} measurements across five replicates. Error bars in the y-direction indicate the experimental uncertainty as discussed in the Supporting Information.

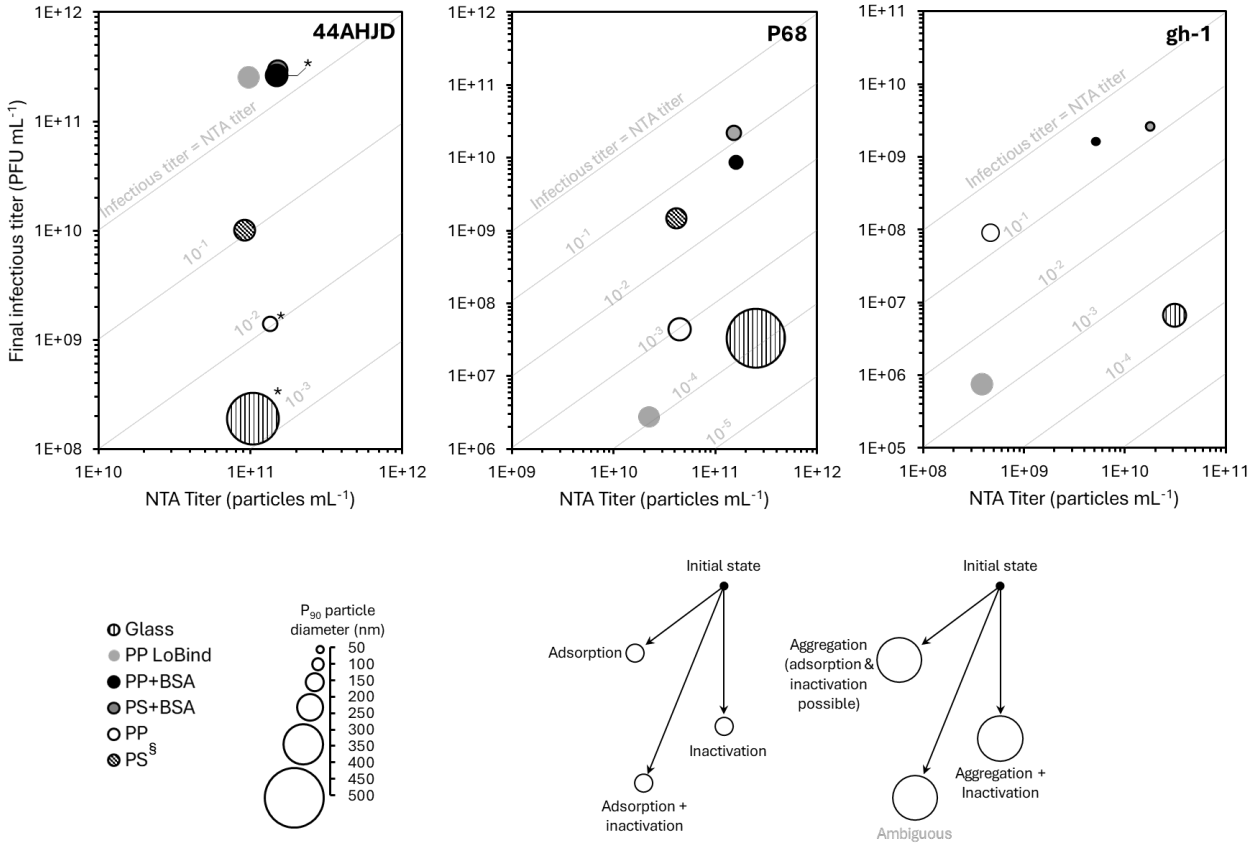

Figure 4 Log-log bubble plots of total particle concentration (x-axis; as measured by nanoparticle tracking analysis) vs. final infectious titer (y-axis; as measured by plaque counting) for all three phages after two weeks in storage in various containers. Datapoint diameters are scaled based on the 90th percentile of particle diameter (*i.e.*, P_{90}) for that suspension as observed by nanoparticle tracking analysis. Diagonal contour lines represent the ratio of concentration of total particles to infectious particles (*i.e.,* suspensions on the 10^{-n} contour feature one infectious particle for every 10^{n} particles). Infectious titers at t=0 were 8.9-18×10^{11} PFU mL^{-1} (44AHJD), 8.3-13.4×10^{11} PFU mL^{-1} (P68), and 1.35-12.5×10^{10} PFU mL^{-1} (gh-1).

§PS-stored gh-1 was too low titer for NTA analysis.
*Indicates containers that were also analysed by SEM.

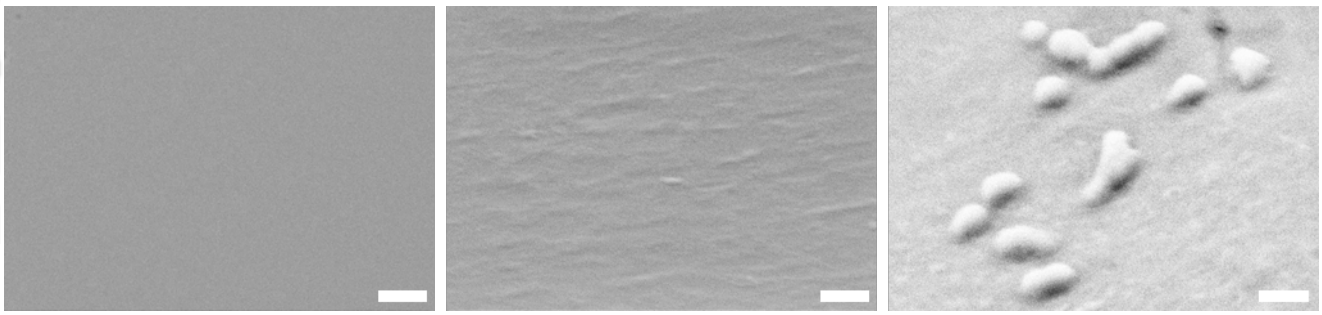

Figure 5 Scanning electron micrographs of glass container inner surface (left), polypropylene (centre), and BSA-treated polypropylene (right). All three containers had been used to store suspensions of phage 44AHJD. Glass was overall much smoother than either bare or BSA-treated polypropylene. In comparison, bare polypropylene appears rougher, and BSA-treated surfaces were rougher still. Increasing surface roughness correlated with improved retention of infectious titer. Particles resembling phages and phage aggregates were observed only on BSA-treated polypropylene. Scale bars indicate 200 nm.

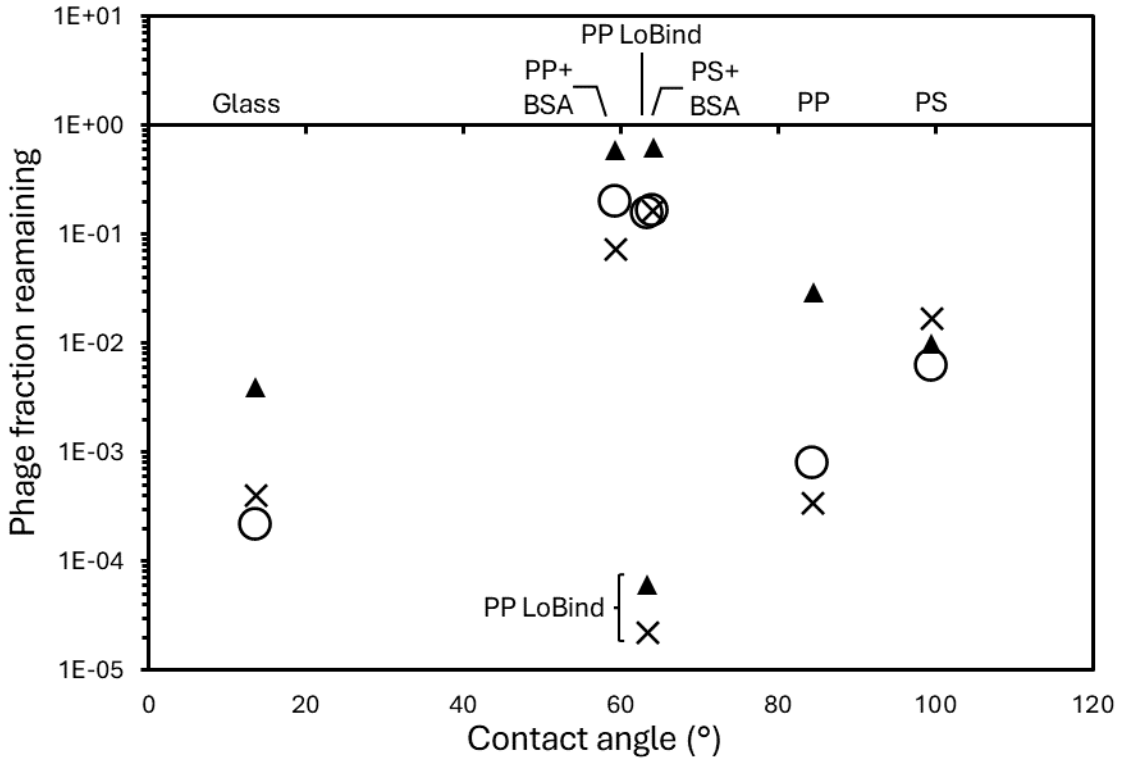

Figure 6 Semilog scatter plots of the fraction remaining of original infectious titer as a function of container contact angle after 0, 1, 7, and 14 days for phages 44AHJD (left), P68 (centre), and gh-1 (right); after storage at 4 °C in glass (◆), polypropylene (■), BSA-treated polypropylene (□), low-binding polypropylene (●), polystyrene (▲), and BSA-treated polystyrene (△).

Supporting Information

One table and one figure concerning correction factors to account for overlap bias in phage plaque-counting, one table summarizing all infectious titer results, and one table summarizing water contact angle measurements are available in supporting information.

Table S1 Summary of spot diameters, plaque diameters, and assay constants (K) for each phage.

Figure S1 Semilog plot showing nominal dilution factor (■) and propagation of uncertainty in dilution factor relative to the parent suspension for glass, PP, and PP+BSA containers (●); and PS and PS+BSA containers (▲), as a function of serial dilution number.

Table S2 Summary table of infectious titer loss for phages 44AHJD, P68, and gh-1; after storage in various labware for 1, 2, 7, and 14 days.

Table S3 Summary table of water contact angle measurements performed on each container type, collated with log10 of infectious titer loss of each phage following 14 days of storage